

# Upwelling : dynamics and consequences on the biological systems

Maria Isabel dos Santos Barros  
Marin Ménard

## Abstract

Upwelling dynamics is investigated through simple theoretical developments, sustained by numerical experiments. Biological consequences are also studied. The example of the Oman coast has been chosen to illustrate the role of wind stress in coastal upwelling, and a simulation in the Gulf Stream region is used to question the theoretical arguments developed for eddy pumping.

## 1 Theoretical background

**Upwelling** is a process in which water masses from deeper layers raise to surface or sub-surface to replace the ones at surface that were dislocated. Ocean waters are affected by the wind on

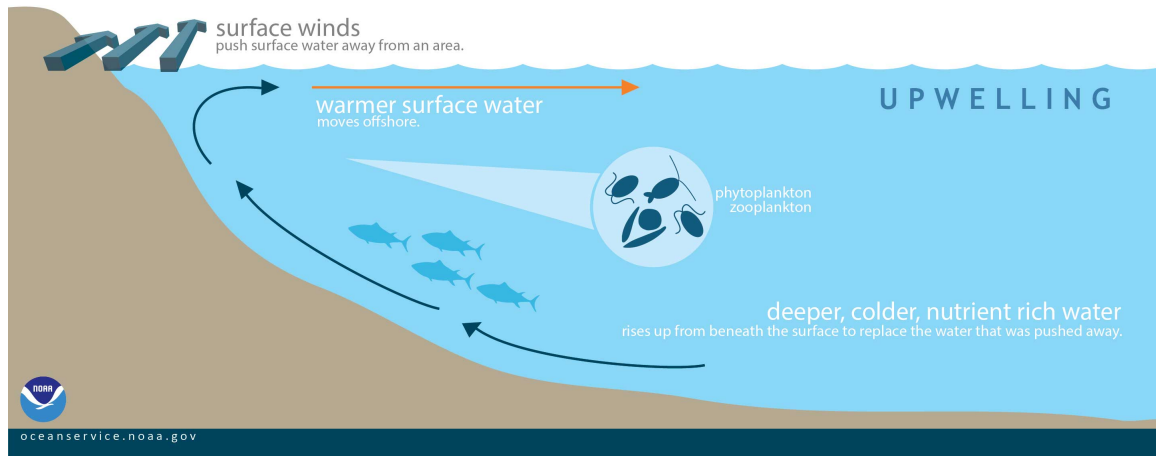


Figure 1: Schematics of the coastal upwelling process

the surface through friction. The momentum from the wind is transferred to the upper layer, the frictional boundary layer or Ekman layer, where there is horizontal frictional stress. In this study, we will consider mesoscale phenomenons in the  $f$ -plane. As the Rossby number is small, we don't consider the material derivative. The horizontal momentum equations for the surface Ekman layer are:

$$-f_0(v - \bar{v}) = \nu_E \frac{\partial^2 u}{\partial z^2} \quad (1)$$

$$f_0(u - \bar{u}) = \nu_E \frac{\partial^2 v}{\partial z^2}, \quad (2)$$

where  $\nu_E$  is the turbulent viscosity coefficient,  $\bar{u}$  and  $\bar{v}$  are the geostrophic interior flow. At the surface, the frictional term is given by:

$$\nu_E \frac{\partial u}{\partial z} = \tau^x \quad (3)$$

$$\nu_E \frac{\partial v}{\partial z} = \tau^y, \quad (4)$$

where  $\tau^x$  and  $\tau^y$  are the zonal and meridional components of the wind stress. If we integrate the velocities  $u$  and  $v$  in depth, considering no topography, we obtain the horizontal transport generated by the wind as given below:

$$U = \int_{-\infty}^0 (u - \bar{u}) dz = \frac{1}{\rho_0 f_0} \tau^y \quad (5)$$

$$V = \int_{-\infty}^0 (v - \bar{v}) dz = -\frac{1}{\rho_0 f_0} \tau^x \quad (6)$$

From that we can conclude that the integrated transport is 90° to right of the wind stress, in the Northern Hemisphere. Vertically integrated divergence in the Ekman layer will get us the Ekman pumping, the vertical velocity that compensates the curl of the wind stress.

$$w_{ek} = \int_{-\infty}^0 \left( \frac{\partial u}{\partial x} + \frac{\partial v}{\partial y} \right) dz = \frac{1}{\rho_0 f_0} \left( \frac{\partial}{\partial x} \tau^y - \frac{\partial}{\partial y} \tau^x \right) \quad (7)$$

Negative wind stress curl will lead to convergence of waters, and consequently downwelling. Whereas positive stress curl leads divergence of waters and upwelling.

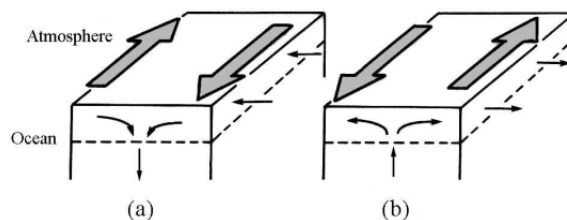


Figure 2: Ekman pumping representing (a) downwelling in case of convergence on the water transport and (b) upwelling in case of divergence of the water transport. This scheme is representative of the Northern Hemisphere. From:[1]

## 1.1 Coastal Upwelling

Coastal upwelling happens when the wind blows parallel to a coast on its left (in the Northern Hemisphere), which creates a divergent Ekman drift and an offshore flow (see figure 1). This drift and the presence of a lateral boundary results in a onshore movement of waters in lower layers and a consequently upward movement to take place of the surface waters. In the ocean important areas of coastal upwelling are called Eastern Boundary Upwelling Systems (EBUS). The four major ones are the Peru-Chile, Canary, Benguela and California upwelling systems. These areas are under the effect of the trade winds, that blow equator-ward on both hemispheres. In the Northern Hemisphere the trade winds blow to the south, so the wind stress parallel to the west coast of the continents (California and Canary systems) generates transport offshore and consequently upwelling [4].

## 1.2 Eddy pumping

Eddies are persistent closed circulations. A cyclone, our focus in this work, rotates at the same sense of the earth rotation, counterclockwise for the Northern Hemisphere [1]. The Ekman pumping induced by the eddy can be calculated from the curl of surface stress, as shown in equation 7. This curl of the surface stress can also be replaced on the equation by the curl of surface currents (relative vorticity). The counterclockwise movement indicates positive curl, which considering  $f > 0$  in the Northern Hemisphere, results in positive vertical velocities and, consequently, upwelling (fig. 3). On the other hand, anticyclones have clockwise motion, negative curl, and a negative vertical velocity as results. This can be observed also in the isopycnals distribution, a cyclone will cause them to go upward and an anticyclone will have the opposite effect [3].

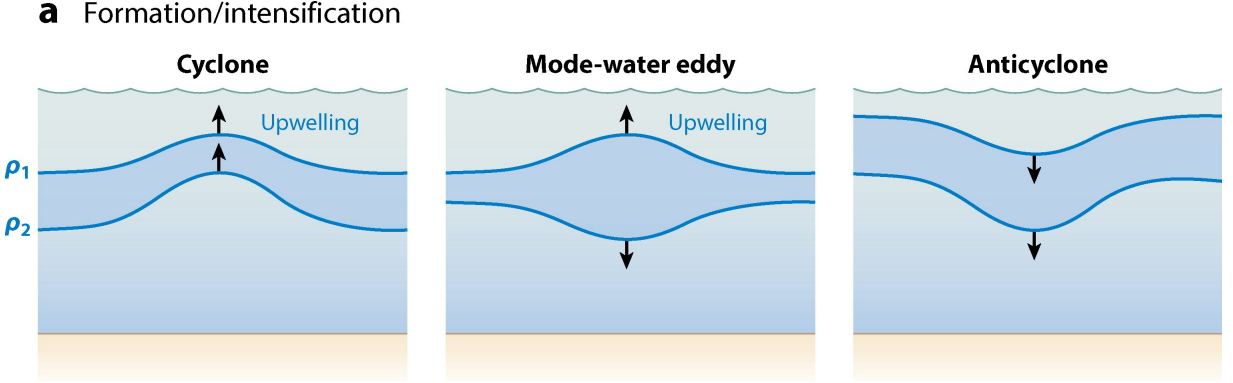


Figure 3: Scheme of the effect of three types of mesoscale eddies on the seasonal (upper isoline of density) and permanent (lower isoline of density) thermocline. On the left, the resulting doming upward of the seasonal thermocline from a cyclone. The second is a mode water eddy that causes both upwelling of the seasonal thermocline and downwelling of the permanent thermocline. The third represents the downward movement of the isopycnals from anticyclones. From: [3]

## 1.3 Eddy-wind interaction

When there's presence of a wind blowing and eddies, the surface stress curl will be affected by the currents generated by the eddies [2]. The equation for  $w_{ek}$  then becomes:

$$w_{ek} = \frac{1}{\rho_0} \nabla \times \left[ \frac{\tau}{(f + \zeta)} \right] \quad (8)$$

$$w_{ek} = \frac{\nabla \times \tau}{\rho_0} \frac{1}{(f + \zeta)^2} \left( \tau^x \frac{\partial \zeta}{\partial y} - \tau^y \frac{\partial \zeta}{\partial x} \right), \quad (9)$$

$$(10)$$

where  $\zeta$  is the local vorticity from the eddy surface currents. The  $\tau$  components are calculated considering the relative velocity between the surface current on the eddy and the wind speed. For a constant zonal wind, one side of the eddy will be aligned to the wind and the other will be in opposition to it (see figure 4). The total eddy pumping then is negative on cyclones(downwelling) and positive in anticyclones(upwelling) in their center. For example, in the case of the easterlies blowing over a cyclonic eddy, on the northern side of the eddy the wind stress will be lower, since both wind and surface currents are on the same direction. On the Southern part the opposite happens : the surface current is contrary to the wind blowing, resulting in stronger wind stress. The transport on both sides is to the right of the wind (northward) but on the Northern side,

the transport is weaker, so there is convergence on the center of the eddy, leading to downwelling movement.

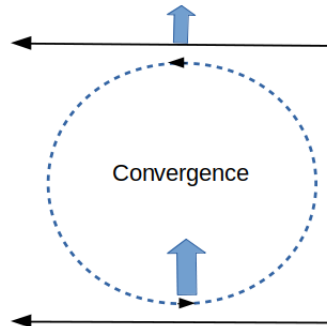


Figure 4: Scheme showing the effect of uniform easterlies on a cyclone in the Northern hemisphere, resulting in downwelling on its center. Adapted from: [3]

## 1.4 Effect on the organisms

Upwelling plays an essential role in biology. Upwelling zones are the ones with the most important biological activity. Phytoplankton is the basis of all the food chain in the ocean, being responsible for the primary production : through photosynthesis, it transforms inorganic matter into organic matter, which can be then consumed by the smallest animal species. Because photosynthesis needs light to occur, phytoplankton is essentially concentrated in the upper layer of the ocean. Indeed, most of the light is absorbed deeper than a few hundreds meters in the ocean. This upper layer where there is still light is called the euphotic zone. It is in this zone that primary production occurs, and where all the animal species feed themselves.

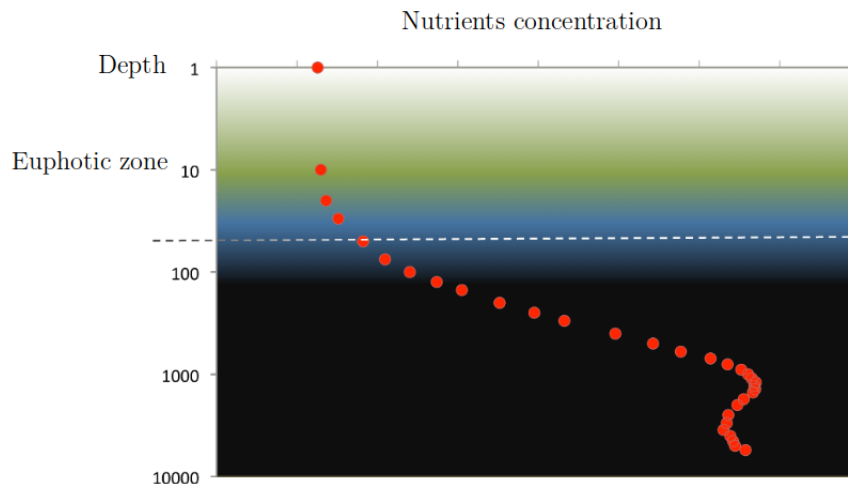


Figure 5: Typical profile of nutrients concentration.

Nutrients have all the same vertical distribution, represented in figure 5. Their concentration decreases at the surface, due to primary production. Phytoplankton uses these nutrients to create organic matter necessary to living organisms. Because of this interaction between the population of

phytoplankton and the nutrients concentration, both reach an equilibrium. Upwelling enable deep nutrients to come up to the euphotic zone. The more concentration of nutrients, the more intense the biological activity. It explains why the upwelling zones are also great fishery zones. It is very important for biologists to improve their knowledge on upwelling dynamics as they are essential to understand the evolution of the different marine species.

## 2 Experimental setup

### 2.1 Coastal upwelling

Two different two-year-long simulation along Oman coast have been performed to show the coastal upwelling occurring in this region. The resolution of the first simulation, called LARGE, is  $1/5^\circ$  ( $\sim 22$  km) for a grid with dimensions  $8^\circ \times 11^\circ$ . This resolution is small enough to resolve the coastal upwelling, but density sections on this simulation present too many artefacts. It has been chosen to run a second simulation, called SMALL, on a smaller domain with a resolution of  $1/15^\circ$  ( $\sim 7$  km). For both simulations, wind forcing varies continuously, interpolating in time the two monthly-mean climatology in between. The drag coefficient  $C_D$  to convert the wind stress to a velocity at 10 m above the surface has been chosen to be  $10^3$ [6]. Salinity and temperature are set from climatology for the beginning of the simulation, but also for the boundary conditions. Lands data is set to zero for every variable (no slip), and tides are not simulated.

### 2.2 Eddy pumping

A third simulation, called GS, has been used to show vertical velocity in an eddy. It is a simulation of the Gulf Stream before Cape Hatteras, where it still flows along the American continental slope. Resolution has been chosen to be  $1/10^\circ$  ( $\sim 10$  km), which is small enough to resolve mesoscale eddies. Again, wind forcing and boundary conditions are imposed by climatology, and tides are not considered. For all the simulations, spin-up has been evaluated from the surface kinetic energy integrated over the domain<sup>1</sup>. To be sure that we get rid of this period, we chose to show the results of the second year of the simulations, which is indicated by the "+1" notation.

## 3 Results

### 3.1 Coastal upwelling

**Wind forcing** Northern Indian Ocean has the particularity of being closed on its Northern boundary, which is very low ( $\sim 25^\circ$ ) compared to the other boundaries. As a subtropical gyre can't be generated, the circulation is quite altered compared to the Pacific or the Atlantic. It is dominated by the monsoon regime. In Summer, the Indian and Bangladesh lands are warmer than the ocean. It creates a large scale thermal wind blowing from the ocean (Southwest) towards the coast (Northeast). This seasonal variability of the wind forcing induces a variability of a lot of phenomenons in the Northern Indian Ocean. For example, the Somali current flows towards the Northeast in summer and towards the Southwest in winter. Figure 6 illustrates the monthly-mean wind forcing, in February (a) and in August (b). In the simulation, wind forcing respects this seasonal variability, as it is derived from climatology data. The wind in August is stronger than in winter, which is also expected, as the Southwest monsoon is more intense than the Northeast one.

**Sea surface temperature** In the Arabian Sea, along the Oman coast, wind blows with the coast on its left in summer. As it is in the Northern hemisphere, the theoretical arguments developed in section 1.1, but also observations, make us expect an important seasonal upwelling. Figure 7

---

<sup>1</sup>See figures 12, 13, and 14 in annexes for more details.

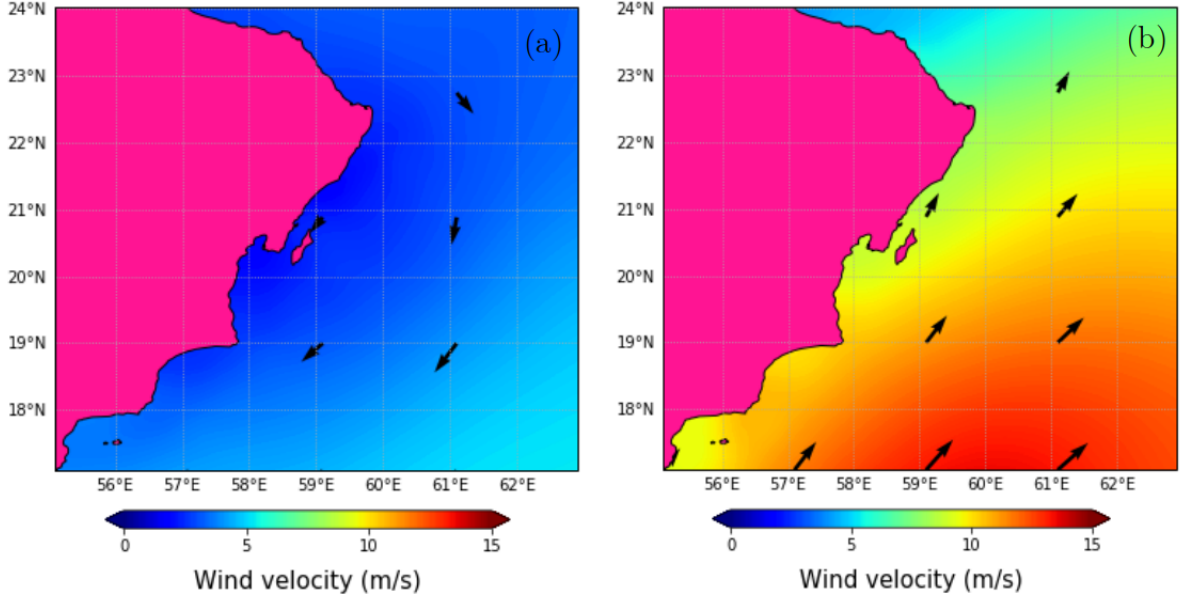


Figure 6: Monthly-mean wind velocity ten meters above the surface for (a) February +1 (Northeast monsoon), (b) August +1 (Southwest monsoon) in the LARGE simulation. Arrows indicate the direction of the wind, and colors its amplitude in m/s.

shows the monthly-mean sea surface temperature (SST) for February +1 (a) and August +1 (b), where upwelling is the most important. SST is clearly more homogeneous in winter than in summer. At the coast, it decreases of  $\sim 4^{\circ}\text{C}$  compared to the offshore water. It is clear that this is due to the coastal upwelling that happens in Summer. Oman upwelling is very singular as it is on the Western

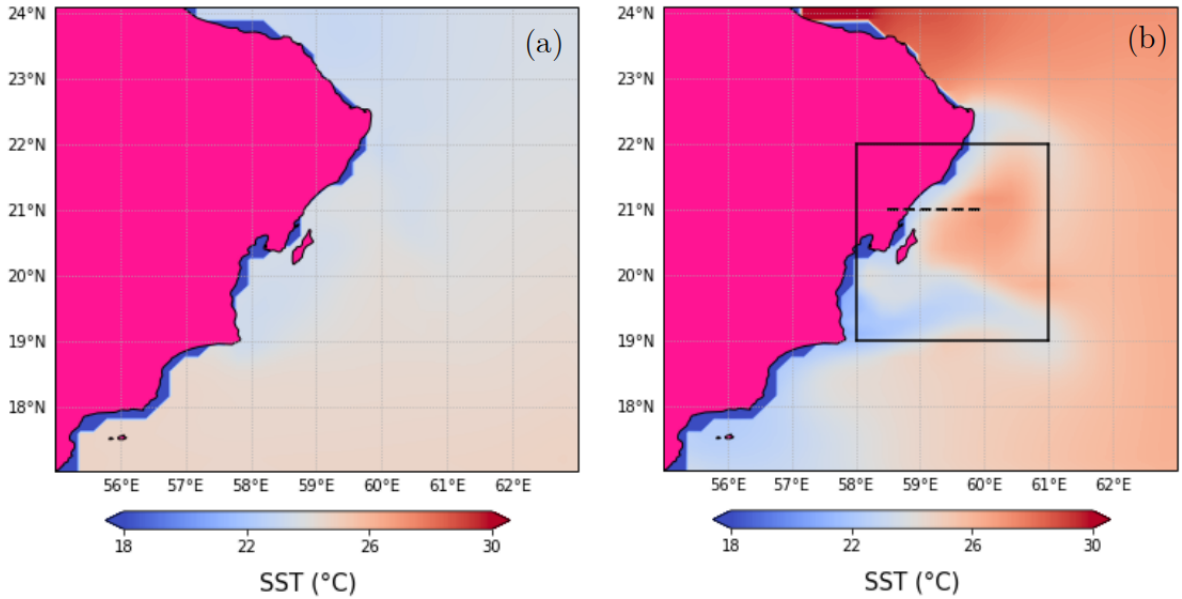


Figure 7: Monthly-mean sea surface temperature for (a) February (Northeast monsoon), (b) August (Southwest monsoon) in the LARGE simulation. Solid rectangle is the domain of the SMALL simulation. Dashed line represents the zonal section used to make figure 8.

boundary of its basin, whereas most of the upwelling systems are localised on Eastern boundaries (EBUS). This particularity is due to the wind forcing, characteristic of the Indian Ocean, imposed by the monsoon regime. This simulation remains quite simplistic as its objective was to show the upwelling happening, but more sophisticated experiments have been made to understand better the dynamics of this region [5].

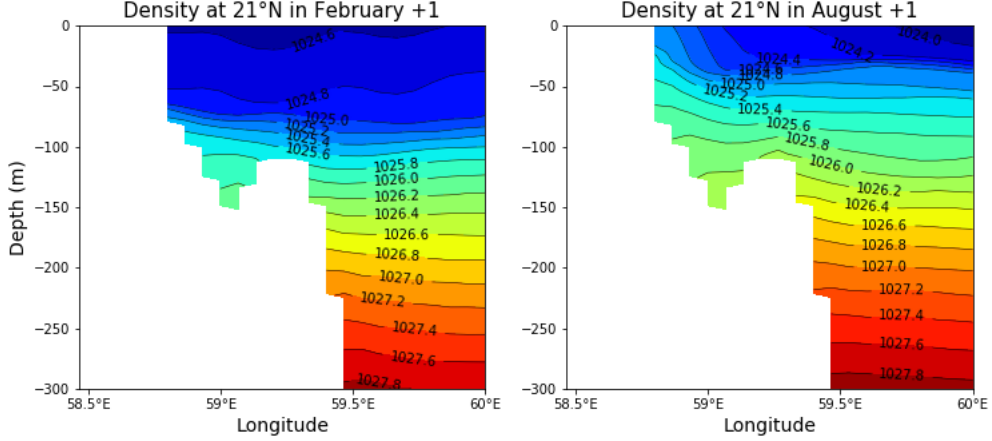


Figure 8: Zonal section of the monthly-mean density at 21°N (see figure 7), in the second year of the SMALL simulation (+1), for February (left) and August (right).

**Zonal section** To illustrate more precisely the Oman upwelling, the SMALL simulation, illustrated in figure 7b with the solid black line, has been used. From its results, a zonal density section has been realised for Northeast and Southwest monsoons. The area is illustrated in dashed line on figure 7b, and results are shown on figure 8. In February, isopycnals are approximately flat. The mixed layer depth is around 70 m as the isopycnals are quite far from each other above this depth. The sharpest gradient, corresponding to the thermocline, is just below this depth. In August, the mixed layer depth tends to be smaller ( $\sim 30$  m), with the thermocline just below. As it is observed on figure 7, SST decreases at the coast. Because temperature drives density at first order, isopycnals rise up to the surface, which shows that denser water masses are present at the surface near the coast. These denser waters are originally below the mixed layer, and also below the euphotic zone. They are then full of nutrients (see figure 5), which enable a stronger primary production, so a stronger biological activity.

### 3.2 Eddy pumping

The GS simulation was used to illustrate eddy pumping. Around the Gulf Stream, eddies are formed as both barotropic and baroclinic instabilities take place. We chose to focus on one cyclonic eddy in this simulation, shown in figure 9. This eddy is over the continental shelf, so there is no major bathymetry effect in this region.

**Vertical structure** To show the vertical velocity in the eddy, a zonal profile is first shown in figure 10. The cyclonic eddy seems to create a downwelling on its core, but an upwelling on its borders. On the Eastern side of the eddy, the pumping is quite strong, with velocities of  $\sim 0.1$  mm/s. With such typical velocities, nutrients which are below 100 m come up to the surface in around 12 days. In our simulation, the eddy is stationary for around  $\sim 15$  days, which enables a lot of nutrients to be brought up to the euphotic zone. However, a large part of the section, especially

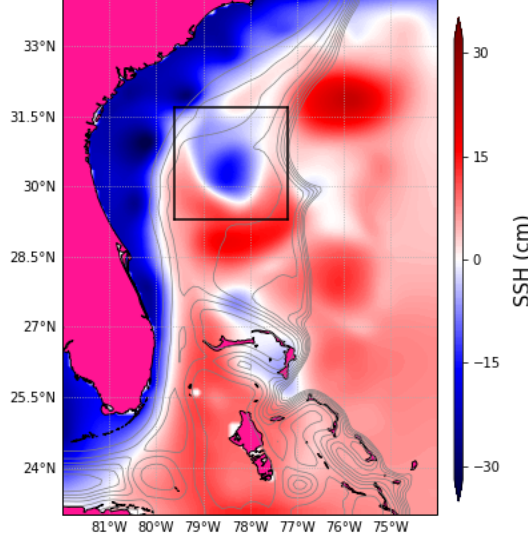


Figure 9: Sea surface height for GS after 8 months of simulation. The solid-black-line domain represents the zoom on the large cyclone on which are computed results presented in figures 10 and 11. Grey thin lines are isobaths between 0 and 2000 m.

near the core, shows a downwelling instead of the upwelling awaited. This is probably due to the wind stress, relatively uniform over the domain, which creates a downwelling inside the cyclone (see section 1.3 and last paragraph for more explanations).

**Horizontal structure** To show the effects of the wind on the vertical velocity, we present in figure 11 the vertical velocity at 100 m depth, associated with the wind stress curl at 10 m above the surface. This depth has been chosen as it is a typical depth below which most of the light is already absorbed, so it can be seen at the boundary of the euphotic zone. Red areas ( $w > 0$ ) correspond to nutrients coming inside this zone. As explained in section 1.2, positive velocities are expected in a cyclone's core without wind stress. Indeed, a cyclonic eddy makes isopycnals rise, and the water masses flow along isopycnals in first order. Furthermore, the wind stress curl is positive all over the domain, which should induce a positive Ekman pumping, considering equation (7). In fact, as the wind is almost uniform, the wind stress curl amplitude is small, so the essential Ekman pumping is due to the eddy structure itself. But in our case, a large part of the domain has negative values, despite the presence of the cyclone. Again, it is probably due to the wind stress that creates a downwelling in the cyclone's core. Wind blows essentially westward, so in the same direction as the Northern part of the cyclone, and in the opposite direction of the Southern part. The difference between Southern and Northern Ekman transports leads to a downwelling, which can compensate the upwelling due to the cyclonic circulation (see figure 4). The more intense the wind, the stronger the downwelling.

Nevertheless, wind stress is not completely uniform. It is a bit stronger on the Northern side of the cyclone. It is increased of  $\sim 0.5$  m/s, which is in the range of velocities encountered in



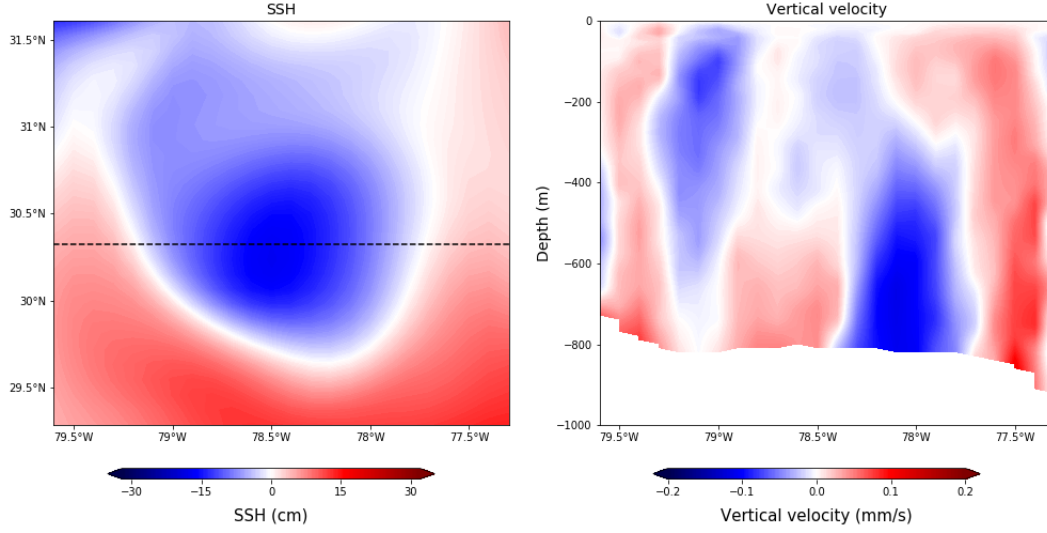


Figure 10: Sea surface height on the domain illustrated in figure 9 (left). The dashed line illustrates the zonal section used to plot the vertical velocity field (right).

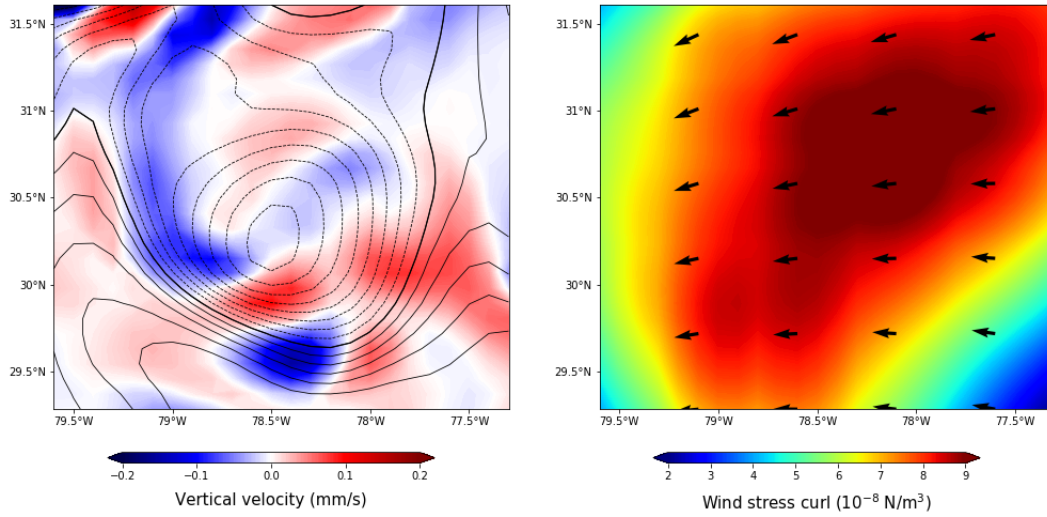


Figure 11: On the left, vertical velocity at 100 m depth, with contours of SSH at each 2 cm. Solid lines are positive values of SSH, and dashed lines are negative. The thicker line represents the 0 cm-level. On the right, arrows illustrated the wind at 10 m above the sea surface, and background corresponds to the wind stress curl.

the cyclone. The effect described previously is then less important, which leads us to expect also positive vertical velocities. However, both effects are in competition, and this is probably why we get a complex structure which is not really consistent with the cyclone shape, illustrated here with SSH contours, or the wind stress curl. But it is clear that eddies create density anomalies that enable to transfer nutrients stuck in the deep ocean to the euphotic zone. In such regions where coastal upwelling can't occur, eddies are essential to biological systems, as they are the main source of nutrients at mesoscale.

## 4 Conclusion

Vertical motions in the ocean are essential to inject the nutrients necessary to primary production. The Oman coastal upwelling is responsible for the large amount of fishery resources in this region. It is more subject to seasonal variability than Eastern Boundary Upwelling Systems. At the beginning of Summer, the ocean becomes more stratified and winds starts blowing from the southwest. Each event encourages blooms to occur. But in regions where there is no upwelling, eddies are the main mesoscale structures that enable nutrients to come to the euphotic zone. We haven't been able to show experimentally the upwelling properties of cyclones. We explain it by not considering air-sea interactions in the theory whereas they are important in the simulation. With more time, it would have been relevant to make a simulation without wind forcing. However, we showed that vertical velocities encountered in cyclones are large enough to enable nutrients to go in the euphotic zone.

## References

- [1] Benoit Cushman-Roisin and Jean-Marie Beckers. “Chapter 8 - The Ekman Layer”. In: *Introduction to Geophysical Fluid Dynamics*. Ed. by Benoit Cushman-Roisin and Jean-Marie Beckers. Vol. 101. International Geophysics. Academic Press, 2011, pp. 239–270. DOI: <https://doi.org/10.1016/B978-0-12-088759-0.00008-0>. URL: <https://www.sciencedirect.com/science/article/pii/B9780120887590000080>.
- [2] Peter Gaube et al. “Satellite Observations of Mesoscale Eddy-Induced Ekman Pumping”. In: *Journal of Physical Oceanography* 45.1 (1Jan. 2015), pp. 104–132. DOI: 10.1175/JPO-D-14-0032.1. URL: <https://journals.ametsoc.org/view/journals/phoc/45/1/jpo-d-14-0032.1.xml>.
- [3] Dennis J. McGillicuddy. “Mechanisms of Physical-Biological-Biogeochemical Interaction at the Oceanic Mesoscale”. In: *Annual Review of Marine Science* 8.1 (2016). PMID: 26359818, pp. 125–159. DOI: 10.1146/annurev-marine-010814-015606. eprint: <https://doi.org/10.1146/annurev-marine-010814-015606>. URL: <https://doi.org/10.1146/annurev-marine-010814-015606>.
- [4] Lynne D. Talley et al. “Chapter 7 - Dynamical Processes for Descriptive Ocean Circulation”. In: *Descriptive Physical Oceanography (Sixth Edition)*. Ed. by Lynne D. Talley et al. Sixth Edition. Boston: Academic Press, 2011, pp. 187–221. ISBN: 978-0-7506-4552-2. DOI: <https://doi.org/10.1016/B978-0-7506-4552-2.10007-1>. URL: <https://www.sciencedirect.com/science/article/pii/B9780750645522100071>.
- [5] Clément Vic et al. “Western boundary upwelling dynamics off Oman”. In: *Ocean Dynamics* 67.5 (2017), pp. 585–595.
- [6] Iwona Wróbel-Niedźwiecka, Violetta Drozdowska, and Jacek Piskozub. “Effect of drag coefficient formula choice on wind stress climatology in the North Atlantic and the European Arctic”. In: *Oceanologia* 61.3 (2019), pp. 291–299. ISSN: 0078-3234. DOI: <https://doi.org/10.1016/j.oceano.2019.02.002>. URL: <https://www.sciencedirect.com/science/article/pii/S0078323419300235>.

## Annexes

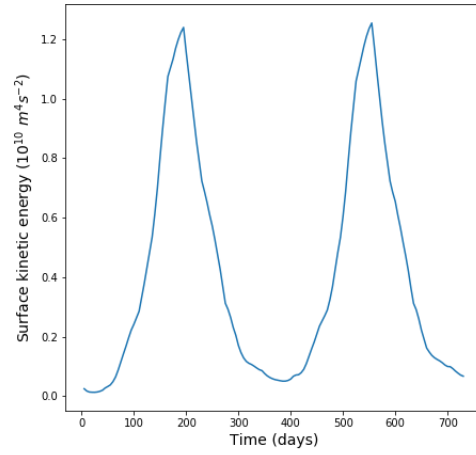


Figure 12: Surface kinetic energy integrated over the domain for the LARGE simulation.

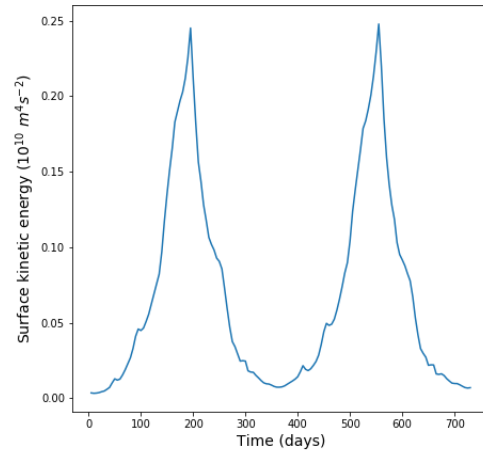


Figure 13: Surface kinetic energy integrated over the domain for the SMALL simulation.

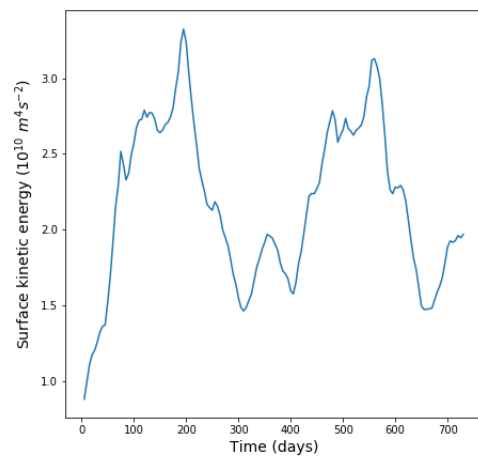


Figure 14: Surface kinetic energy integrated over the domain for the GS simulation.